

Yale University

## EliScholar – A Digital Platform for Scholarly Publishing at Yale

---

Yale Medicine Thesis Digital Library

School of Medicine

---

2003

# Developing anti-CD30 recombinant immunotoxins targeting shed and non-shed epitopes for cancer therapy

Abhishek Sinha

Follow this and additional works at: <http://elischolar.library.yale.edu/ymtdl>



Part of the [Medicine and Health Sciences Commons](#)

---

### Recommended Citation

Sinha, Abhishek, "Developing anti-CD30 recombinant immunotoxins targeting shed and non-shed epitopes for cancer therapy" (2003). *Yale Medicine Thesis Digital Library*. 3352.  
<http://elischolar.library.yale.edu/ymtdl/3352>

This Open Access Thesis is brought to you for free and open access by the School of Medicine at EliScholar – A Digital Platform for Scholarly Publishing at Yale. It has been accepted for inclusion in Yale Medicine Thesis Digital Library by an authorized administrator of EliScholar – A Digital Platform for Scholarly Publishing at Yale. For more information, please contact [elischolar@yale.edu](mailto:elischolar@yale.edu).

MED  
T113  
+Y12  
7050

Developing Anti-CD30 Recombinant Immunotoxins  
Targeting Shed and Non-Shed Epitopes for Cancer Therapy

---

Abhishek Sinha

YALE UNIVERSITY

2003


YALE  
UNIVERSITY



CUSHING/WHITNEY  
MEDICAL LIBRARY







Digitized by the Internet Archive  
in 2017 with funding from  
The National Endowment for the Humanities and the Arcadia Fund

<https://archive.org/details/developingscalet00fast>



**Developing Anti-CD30 Recombinant Immunotoxins Targeting Shed and  
Non-Shed Epitopes for Cancer Therapy**

**A Thesis Submitted to the  
Yale University School of Medicine  
in Partial Fulfillment of the Requirements for the  
Degree of Doctor of Medicine**

**by  
Abhishek Sinha  
2003**



YALE MEDICAL LIBRARY

AUG 11 2003

T 113  
+ Y 12  
7050

## Developing Anti-CD30 Recombinant Immunotoxins Targeting Shed and non-Shed Epitopes for Cancer Therapy

Abhishek Sinha, Richard Beers, Satoshi Nagata, Tapan Bera, Masanori Onda, Kenneth Santora, Ira Pastan. Laboratory of Molecular Biology, National Cancer Institute, National Institute of Health, Bethesda, MD 20892. (Sponsored by Vincent DeVita, Yale Cancer Center, Yale University School of Medicine).

Although combination chemotherapy and radiation therapy achieves high remission rates in patients with Hodgkin's disease (HD) and some forms of Anaplastic Large Cell Lymphoma (ALCL), most patients who relapse will die of their disease. Also, approximately 20% of long term survivors of HD who receive chemotherapy and radiation therapy develop secondary malignancies, which further underlines the need for more selective therapeutic agents. CD30, a 120 kd transmembrane protein of the TNF receptor family, is a human lymphocyte activation antigen that is consistently over-expressed in Reed Sternberg cells (HD) and in ALCL cells, yet it is poorly expressed on normal lymphocytes, making it an ideal target for selective immunotherapy. Recombinant immunotoxins (RITs) genetically fuse the Fv (variable region) of a monoclonal antibody (MAb) targeting a surface tumor antigen with a modified form of the *Pseudomonas* exotoxin, combining the specificity of an antibody with the powerful cytotoxicity of a bacterial toxin. To develop anti-CD30 RITs, four new high affinity anti-CD30 antibodies (T420, T427, T405, T105) targeting different epitope groups were selected from a panel of anti-CD30 MAbs. Because part of CD30 is cleaved into a soluble fragment, it is important to design RITs that target the shed and non-shed CD30 epitopes. After cloning and sequencing the variable regions of these MAbs, separate expression constructs were made for the light chains ( $V_L$ ) and the heavy chains fused to the *Pseudomonas* exotoxin ( $V_H + PE38$ ). After expressing, refolding, and purifying the RITs, each RIT's specific cytotoxicity was evaluated in various CD30+ cell lines. Three of RITs demonstrated high degrees of specific cytotoxicity towards CD30+ cells in *in vitro* assays, with  $IC_{50}$ 's as low as 0.63 to 2.0 ng/ml. RITs with the highest activities will be further characterized, and the RIT with the most favorable properties may be a candidate for development for clinical trials.



## **Acknowledgements**

I would like to thank Dr. Ira Pastan, M.D., not only for the opportunity to pursue this project but for all of his guidance, support, and mentorship throughout it. I would also like to thank other members of the Pastan lab. In particular, I would like to thank Richard Beers and Satoshi Nagata for their invaluable help, advice, and friendship during this project. In addition, I want to thank Tapan Bera and Mansanori Onda for their helpful advice.

I would especially like to thank Dr. Vincent DeVita, M.D., for sponsoring my project and for all of his helpful advice and insight during the writing of my thesis.

This work was supported by the HHMI-NIH Research Scholars Program.



## Table of Contents

1. Abstract .....	p. 2
2. Acknowledgements .....	p. 3
3. Introduction .....	p. 5
4. Statement of Purpose and Hypothesis .....	p. 9
5. Methods .....	p. 10
6. Results .....	p. 16
7. Discussion .....	p. 20
8. References .....	p. 26
9. Figures and Tables .....	p. 31



## **Introduction:**

Combination chemotherapy and radiation therapy can cure a substantial fraction of patients with Hodgkin's Disease (HD) (1). In the advanced stages of the disease, approximately 30 to 50% of patients will respond to therapy but relapse and die of this disease (2). Overall, 20% of patients with Hodgkin's disease die as a result of their illness (3). In addition, conventional therapy for Hodgkin's disease leads to several co-morbidities. Long-term survivors of Hodgkin's Disease who received chemotherapy and radiotherapy have a higher risk of developing a secondary malignancy. The possible secondary malignancies include myelodysplastic syndromes, AML, lung cancer, NHL, breast cancer, gastric cancer, sarcoma, and malignant melanoma (4). Women who are treated with radiation therapy to the chest during adolescence are especially at risk for developing breast cancer (5). Approximately 19% of long term survivors of Hodgkin's disease receiving chemotherapy and radiotherapy will develop a secondary malignancy after 15 years from their treatment. Other complications of radiotherapy include pulmonary fibrosis and accelerated atherosclerosis. The poor prognosis in patients who relapse and the co-morbidities of patients receiving combinational chemotherapy and radiotherapy underlie the need for more selective therapy in Hodgkin's Disease.

Anaplastic large cell lymphoma (ALCL), a novel category of lymphoma (categorized in 1985) that has a cohesive proliferation of large pleomorphic blastic cells and consistently expresses the cytokine receptor CD30, can be clinically divided into a primary systemic form, a primary cutaneous form, and a secondary form (6,7). The most common subform is the primary systemic form which can account for 2 to 8% of non-Hodgkin's lymphomas in adults and about 20-30% of large cell lymphomas in children (7). It is worth noting that





because ALCL has been recognized relatively recently and in the past has been misdiagnosed (as malignant histiocytic tumors, regressing atypical histiocytosis, melanoma, metastatic carcinoma), its true prevalence is unknown. The primary systemic form can also be divided into groups that are anaplastic lymphoma kinase (ALK) positive or negative. Anaplastic lymphoma kinase is a receptor tyrosine kinase. The ALK+ ALCL form presents mostly in the first three decades of life while the ALK- form occurs in older patients (8,9,10). Extranodal involvement is possible in both ALK+ and ALK- subforms (esp. ALK+) and includes skin, bone, soft tissue, lung, liver, and CNS (rare) (11). The prognosis of primary ALCL can also vary depending on the presence of ALK. The 5 year overall survival for ALK+ ALCL is 71% +/- 6% and for ALK- ALCL is 15% +/- 11% (11). The secondary form of ALCL arises from the progression of other lymphomas and is associated with a poor prognosis. While the prognosis of ALCL varies depending on the subforms, there is a clinical need, as in HD, for more selective therapies.

Hodgkin's disease and ALCL are distinct clinical entities, but they share many characteristics. One of the most important of these is that both Reed-Sternberg cells of HD and ALCL cells consistently express CD30, a human lymphocyte activation marker. CD30, a type I transmembrane glycosylated protein of 120/105 kDa, is a member of the TNF receptor (TNFR) superfamily (12,13). CD30 expression in normal cells is restricted to activated lymphocytes and is absent from hematopoietic stem cells. Stimulation of CD30 has been associated with a variety of biological activities in lymphoid cells (depending on the circumstances) including proliferation, activation, differentiation, and cell death (14). It is also known that CD30 cross-linking leads to NF- $\kappa$  B activation (15,16). NF- $\kappa$  B activation (via CD30) is believed to transcriptionally regulate several cellular genes (including various



cytokines) which may explain some of the numerous biological effects of CD30 activation, such as lymphocyte proliferation (17). The extracellular portion of CD30 can also be cleaved by a zinc-metalloprotease to yield a soluble form (sCD30, mass 85/90 kDa) (18). Increased levels of sCD30 have been found in patients with HD and ALCL and correlate with disease burden. In fact, the median sCD30 levels in patient with HD and ALCL were found to be 20 to 1500 times greater than in normal controls (19). Because CD30 expression is restricted to Reed-Sternberg cells, ALCL cells, and some activated lymphocytes and is absent from hematopoietic stem cells, it is an excellent target for selective immunotherapy.

One possible strategy for targeting CD30 is the use of recombinant immunotoxins (RITs). RITs are chimeric proteins that genetically fuse the Fv (fragment of the variable region) of a monoclonal antibody (MAb) that targets a tumor surface antigen with a modified bacterial toxin (or plant toxin) (20,21). Hence, RITs combine the specificity of a MAb with the powerful cytotoxicity of a bacterial toxin (Figure 1). RITs are useful in cases when unarmed MAbs are not able to kill cancer cells, which is often the case. Linking a MAb or Fv of MAb with a toxin (as opposed to cytotoxic drug or radioisotope) has many advantages which include: 1. toxins are highly potent, 2. toxins are not mutagenic, 3. toxins are not toxic to bone marrow, 4. toxins can kill cancer cells that are chemotherapy resistant, 5. It is rare for cells to develop resistance to bacterial toxins. There are several generations and forms of immunotoxins (ITs). The term recombinant immunotoxin is used to signify that the toxin and Fv of the MAb were genetically fused rather than chemically conjugated. The RITs utilize a modified *Pseudomonas* exotoxin which kill cells by ADP ribosylating and inactivating elongation factor 2 (Figure 1a) (20). The RIT binds to its target and enters the cell through an endocytosis pathway. The *Pseudomonas* exotoxin is proteolytically cleaved



and a portion of it is sent to the Golgi and then the endoplasmic reticulum, from where it is translocated to the cytosol. Once in the cytosol, the toxin kills the cell by inhibiting protein synthesis. Clinical trials with other RITs that target other tumor antigens indicate that such therapy may be effective in hematologic malignancies. LMB-2 (anti-CD25 scFv immunotoxin) resulted in significant clinical responses in various types of leukemia and lymphoma (22). In addition, RFB4 (dsFv)-PE38 (the anti-CD22 RIT) was able to achieve high rates of complete remission in patients with Hairy Cell Leukemia refractory to chemotherapy (23,24).

A number of attempts to target CD30 with MAbs and immunotoxins have been made. Some of the earlier MAbs generated to target CD30 are Ber-H2, HeFi-1, M44, M67, and Ki-1 (25). Anti-CD30 MAbs have been shown to induce cell growth inhibition and apoptosis in ALCL (26,27). Mouse models using ALCL xenografts that were treated with the HeFi-1 MAb and the M44 MAb had growth arrests of tumors and increased in survival (27,28). Clinical studies with the Ber-H2 MAb and the HeFi-1 MAb were performed. The Ber-H2 MAb was given to patients (along with a small amount of <sup>131</sup>I-labeled Ber-H2) to patients with refractory Hodgkin's disease. Tumor localization was seen (through radioimaging) in 50% of the tumors, and there was non-specific uptake in the spleen and liver. This study revealed no clinical responses or toxicities. Results of the study with HeFi-1 MAb revealed tumor localization and no responses (25). Recently, a group reports some efficacy of another MAb (SGN-30) on HD in *in vitro* studies and in murine models (29). Immunotoxins targeting CD30 have had some effects in *in vitro* studies and animal models. A RIT that was derived from the Ki-4 MAb and modified *Pseudomonas* exotoxin was shown to have some specific cytotoxicity in *in vitro* studies with CD30+ cells and some anti-tumor activity in a



SCID mouse model (30,31). Clinical studies with a Ber-H2 MAb conjugated to a saporin toxin used in patients with HD revealed greater than 50% reduction in tumor mass, but these responses were temporary (32). Recently, a Phase I study with Anti-CD30 Ricin A-Chain immunotoxin (Ki-4.dgA) had minor clinical responses (1 partial remission in 15 patients) but significant toxicity (33). The Pastan lab has also made several RITs which have shown significant specific activity in both *in vitro* studies and animal models (34,35).

### **Statement of purpose and hypothesis:**

While previous attempts to target CD30 with MAbs and ITs have shown some efficacy in *in vitro* assays and in animal models, producing a RIT with improved properties should result in greater clinical efficacy. Four MAbs (T420, T427, T105, and T405) were selected from a panel of anti-CD30 MAbs recently produced and characterized by affinity assays and CD30 epitope mapping (Figure 2, Table 1). Because a high affinity parent MAb should produce a more active RIT, two of the MAbs (T420 & T427) were selected because of their very high affinities (T420's  $K_d = 1.9$  nM, T427's  $K_d = 0.9$  nM) towards CD30. The epitope the RIT targets may be especially significant because, as mentioned above, the extracellular portion of CD30 is cleaved to yield a soluble fraction (sCD30), and sCD30 levels can be dramatically higher in patients with HD and ALCL. CD30 has multiple epitope groups, some of which are located on the non-shed portion (S. Nagata, unpublished data, Figure 2). The advantage of a RIT that targets a non-shed epitope is that it should have a greater number of available binding sites and should not be neutralized by sCD30. RITs based on T105 and T405 parent MAbs are the first to target non-shed CD30 epitopes.





## METHODS

### **Cloning of $V_H$ (variable region of the heavy chain) and $V_L$ (variable region of the light chain) of the Parent MAbs.**

In order to clone the  $V_H$  and  $V_L$  of the four parent MAbs (T420, T427, T105, T405), the total cellular RNA was extracted from hybridoma cells and used to produce the  $V_H$  and  $V_L$  cDNA through a SMART RACE (Rapid Amplification of cDNA Ends) reaction. The  $V_H$  and  $V_L$  cDNA were then separately cloned into a pCR2.1-TOPO (plasmid) vector. Isolation of total cellular RNA from  $10^7$  hybridoma cells was done with an RNA extraction kit (StrataPrep Total RNA Miniprep Kit, Stratagene Cloning Systems, La Jolla, CA). From each hybridoma total RNA, the cDNA of the  $V_H$  and  $V_L$  of the MAbs (T420, T427, T105, T405) were generated using SMART RACE cDNA Amplification Kit (Clontech, Palo Alto, CA). Essentially a two step process, the first part involved generating adaptor-ligated cDNA through a reverse transcriptase reaction of 5ug RNA using a 3' primer that was derived from the sequence of the constant region ( $C_{HI}$  or  $C_L$ ) or hinge region (for heavy chains only) for that parent MAb. Since different subclasses of immunoglobulins have different constant region sequences, the 3' primers were designed and chosen corresponding subclass of the parent MAb using the Kabat database (Table 1). The 3' primers used were:  $\gamma 1$  (hinge region primer, T105  $V_H$ ) = ACC-ACA-ATC-CCT-GGG-CAC-AAT-TTT-CT;  $\gamma 2a$  (hinge region primer, T427  $V_H$ ) = TCT GGG CTC AAT TTT CTT GTC CAC C;  $\gamma 2b$  (hinge region primer, T420 & T405  $V_H$ ) = GCT GGG CTC AAG TTT TTT GTC CAC C;  $\kappa$  (for all  $V_L$ ) = CTC ATT CTT GTT GAA GCT CTT GAC ATT. The next step involved using the cDNA generated from the reverse transcriptase reaction as a template for a 5' RACE reaction. This reaction used a 5' end primer that binds to the adaptor sequence and a 3' end primer also



derived from the constant region of the appropriate immunoglobulin subclass (but is upstream to the primers used in the first step). These 3' primers for the RACE reaction were:  $\gamma$ 1 (CH1 primer, T105 VH) = CAG GGT CAC CAT GGA GTT AGT TTG,  $\gamma$ 2a (CH1 region primer, T427 VH) = TAG AGT CAC CGA GGA GCC AGT TGT,  $\gamma$ 2b (CH1 region primer, T420 & T405 VH) = TCC AGA GTT CCA AGT CAC AGT CAC,  $\kappa$  (for all VL) = GAC TGA GGC ACC TCC AGA TGT TAA. To purify the products of the 5' RACE reaction, the PCR products were run on 1.2% low melting agarose gel, and bands of the expected product size were excised and purified with Qiaquick gel extraction kit. Using Invitrogen's TOPO TA cloning kit (Invitrogen, San Diego, CA), these purified PCR products were cloned into a pCR2.1-TOPO vector. These clones were then sequenced. To eliminate the possibility that the clone contained a PCR generated error, at least five clones per  $V_H$  or  $V_L$  clone were sequenced. Once the sequences were obtained, they were aligned according to the Kabat alignment scheme (36).

### **Construction of Plasmids for dsFv-PE38 (disulfide-stabilized Fv fragment linked to a modified *Pseudomonas* exotoxin) Recombinant Immunotoxins.**

After cloning and sequencing the  $V_H$  and  $V_L$  of the parent MAb, cysteine (cys) mutations were introduced into the  $V_H$  and  $V_L$  (to form a disulfide bond during the refolding process), and the  $V_H$  w/cysteine and  $V_L$  w/cysteine were incorporated into separate plasmid expression vectors. In the  $V_H$  expression vector,  $V_H$  w/cys is joined to a modified *Pseudomonas* exotoxin that is 38 kDa large (PE38). A cysteine mutation was introduced into the  $V_L$  chain at position 100 (according to Kabat numbering) in framework region 4 (FR4) and into the  $V_H$  chain at position 44 in framework region 2 (FR2) (Figure 3a) (37). To



introduce a cysteine mutation in  $V_L$  and prepare it for ligation into the expression construct, the  $V_L$  chain was PCR amplified with a 5' primer (that introduce an Nde I site) and a 3' primer that introduced a cysteine mutation in position 100 (FR4) and an EcoR1 site. Because a cysteine mutation had to be introduced in the middle (position 44) of the  $V_H$  chain, a splicing overlap extension PCR method was employed (38). This involves PCR amplifying the first half of the  $V_H$  chain with primers that introduce a Nde I site (with an ATG initiation codon) at the 5' end and a cysteine mutation (at position 44) at the 3' end of the fragment. The second fragment of  $V_H$  is produced by PCR amplification with primers that introduce a cysteine mutation at position 44 in the 5' end of the fragment and a Hind III mutation at the 3' end. Because  $V_H$  fragment 1 and fragment 2 overlap (around the cysteine mutation), an overlap reaction produces a  $V_H$  w/cysteine chain by allowing the overlapping ends to anneal and extend. This full length  $V_H$  segment with cysteine is amplified with the 5' and 3' primers. The  $V_L$ (cys) and  $V_H$ (cys) were digested with Nde I and EcoR1 (for  $V_L$ ) or Hind III (for  $V_H$ ). They were then ligated into separate T7-based expression vector pRB98a (which originated from pUL17; 4) (Figure 3b). The  $V_H$  expression vector attaches  $V_H$  (cys) to PE38 (with a small connector region in between) (Figure 3c). The  $V_L$ (cys) is alone in a separate expression vector (Figure 3d). The sequence of the  $V_H$ (cys)-PE38 and  $V_L$ (cys) expression vector were verified.

### **Production and Purification of dsFv Recombinant Immunotoxins (RITs)**

The preparation of recombinant dsFv immunotoxins involved expressing the  $V_H$  (cys)-PE38 and  $V_L$  (cys) (which collect as intracellular inclusion bodies, IB), purifying, solubilizing and denaturing the IB, refolding the IB in a redox-shuffling buffer, a dialysis process, and



column chromatography to separate the refolded dsFv IT from aggregates (39,40). The  $V_H(\text{cys})$ -PE38 and  $V_L(\text{cys})$  expression vectors were separately transfected into *E.coli* BL21 ( $\lambda$ DE3). Protein expression was induced in the bacterial cultures with 1mM isopropyl-1-thio- $\beta$ -D-galactopyranoside for 2 hrs during the exponential growth phase. The cells were collected by centrifugation. The recombinant proteins, which collect as intracellular inclusion bodies, were recovered by lysing the cells. The inclusion bodies were then washed repeatedly with a non-ionic detergent. After washing, the purified inclusion bodies are solubilized and denatured with 6 M guanidine hydrochloride and then reduced by dithioerthritol for approximately 5 hours. After being solubilized and reduced,  $V_H(\text{cys})$ -PE38 and  $V_L(\text{cys})$  were added in a 2:1 molar ratio and diluted (100x) into a redox-shuffling buffer which contains oxidized and reduced glutathione and L-arginine (to help prevent protein aggregation). The refolding process (which takes about 38 to 42 hrs) is followed by dialysis against a Tris buffer (with 0.1 M urea) for approximately 18 hours to remove the guanidine hydrochloride. The refolded, dsFv RIT is then separated from misfolded aggregates and bacterial protein through a series of anion exchange chromatography (Q-Sepharose and then Mono-Q [Amersham Pharmacia Biotech]) and then size exclusion chromatography (TSK3000; TOSOHH, Tokyo, Japan). The refolded dsFv was further analyzed by SDS-Page gel for size and purity. A Bradford assay (Coomassie Plus, Pierce, Rockford, IL) using a BSA standard was used to measure the concentration of the recovered IT.

### **Cell Lines for Cytotoxicity Assays.**

The cell lines used for the cytotoxicity assay include Atac-4 and A431-CD30 (which is a stable transformant of A431 that expresses CD30) (41,42). A431 is a human epidermoid





cell line, and Atac-4 is a stable transformant of A431 that expresses CD25 (but is CD30-). ALCL-derived cell lines were SUDHL-1 and KARPAS-299 (from the German Collection of Microorganism and Cell Cultures, DSMZ, Braunschweig, Germany). L540 was a HD derived cell line (from Dr. C.S. Duckett, NIH, Bethesda, MD). SUDHL-1, KARPAS-299, and L540 cells are all CD30+. Iscove's modified Dulbecco's medium (Life Technologies, Inc., Gaithersburg, MD) was used for culturing the cells.

### **In Vitro Cytotoxicity Assay**

Activity of the RIT is measured by the inhibition of cellular protein synthesis as measured by  $^3\text{H}$ -leucine incorporation (41). Cells are plated in a 96 well plate at  $2.0 \times 10^4$  cells/well. They are then incubated for 24 hrs if the cell line is attached or for 1 hrs if the cells grow in suspension. Serial dilutions of the RIT are made in PBS with 0.2% with human serum albumin. The RIT are added to the cells (3 wells for each RIT dilution) and then incubated for 18-30hrs (the incubation period varies depending on the growth rate of the cell line being tested). After being incubated with the RIT, 2  $\mu\text{Ci}$  of  $^3\text{H}$  Leucine (diluted 1:10 in 0.2% HSA in PBS) is added and incubated with the cells for 2 to 5 hrs. If the cell line used is attached, the plates are frozen and thawed (to disattach the cells from the surface of the 96 well plate). If the cell line grows in suspension, the freezing and thawing step is not necessary. They are then harvested onto glass filters using a cell harvester (Tomtec, Hamden, CT). The incorporation of radioactivity (counts) is measured by an automated scintillation counter (1205 Beta-plate; Wallac, Gaithersburg, MD).



## **Surface Plasmon Resonance Assay**

A BIAcore (Biacore, Piscataway, NJ) biosensor was used to measure the affinity of the dsFv RIT for CD30. To measure the on and off rates, CD30-Fc (4000 resonance units) was affixed to a biosensor chip, and 25 $\mu$ g/ml of an IT (in PBS) was injected over the chip surface for 5min . The RIT was then allowed to dissociate by flowing buffer over the chip. Binding kinetics were measured by using BIAevaluation 2.1 software (BIAcore). [The surface plasmon resonance assay was done largely by Richard Beers]



## **RESULTS:**

### **Cloning of V<sub>H</sub> (variable domain of the heavy chain) and V<sub>L</sub> (variable region of the light chain) cDNA of the Parent MAb**

The cDNA of the V<sub>H</sub> and V<sub>L</sub> domains of each of the MAbs (T420, T427, T105, T405) were cloned as described in “Materials and Methods”. The sequence data were arranged into tables organized by framework regions (FR) and complementary determining region (CDR) (Table 2 ). The amino acid sequences were also analyzed through an “Fv Sequence Alignment “ program (Molecular Modeling Section, Laboratory of Molecular Biology, NCI/NIH) that identifies any unusual residues in the framework region. This is important because unusual amino acids in the framework can prove to be problematic for the stability and activity of the Fv. One interesting anomaly among the V<sub>H</sub> and V<sub>L</sub> sequences was that CDR3 in the V<sub>H</sub> chain for T405 has only three amino acid residues, considerably shorter than most other CDR3s. Otherwise, most of the cloned sequences appeared reasonable.

### **Preparation and Purification of Anti-CD30 dsFv (disulfide-stabilized Fv) Immunotoxin**

The dsFv RITs (recombinant immunotoxin) were produced according to the protocol described in “Materials and Methods”. Cysteine mutations introduced into the V<sub>H</sub>-PE38 and V<sub>L</sub> chains allow them to form a disulfide bond during the refolding process (Figure 1a). The redox-shuffling buffer promotes the formation of the disulfide bond between V<sub>H</sub> and V<sub>L</sub>. This disulfide form of IT was found to be more stable than the single chain form (V<sub>H</sub> and V<sub>L</sub> linked by a peptide) and has greater anti-tumor activity (37,39,43).

Two important criteria for a successful RIT are yield and purity, as dsFv immunotoxins may aggregate during the refolding process (lowering yield and purity). A



low yield indicates that the  $V_H$  and  $V_L$  are not stable in an Fv form. A dsFv RIT that cannot be recovered with good purity will likely have diminished activity because of the contaminants (misfolded protein aggregates). All four anti-CD30 dsFv RIT were made (T420, T427, T105, & T405) with reasonable yields (minimum acceptable yield is 1%, a yield  $\geq 5\%$  is desirable) ( Table 2). Also, all four were produced and recovered with high purity (Figure 4), indicating that their Fvs are relatively stable. Except for T420, the RITs are shown in reducing and non-reducing conditions. In non-reducing conditions, the disulfide bond is cleaved, causing  $V_H$ -PE38 to be separated from  $V_L$ . Since good yields and high purity typically correlate with high activity, all four RITs appeared favorable at this stage.

### **Testing Anti-CD30 RIT for Specific Activity**

The specific activity of the anti-CD30 dsFv RITs were measured by in vitro cytotoxicity assays in CD30+ cell lines. Because the *Pseudomonas* exotoxin's mechanism of killing is through in ADP ribosylation of elongation factor 2, these cytotoxicity assays measure inhibition of cellular protein synthesis as means to determine the activity of the RIT. This inhibition of cellular protein synthesis correlates with cell death. The  $IC_{50}$  of the anti-CD30 dsFv was determined by applying varying concentrations of the RIT to A431/CD30 (see "Materials and Methods"). As a positive control, a potent anti-CD30 dsFv RIT previously made in the lab (T6 dsFv RIT) was included in the assay. To confirm that their cytotoxicity was specific, these anti-CD30 dsFv RIT's were tested in a CD30 negative cell line, Atac4.





The results of the cytotoxicity assay indicate that T420 RIT, T105 RIT, and T427 RIT were all highly active against CD30+ cells (with  $IC_{50}$  in the 0.63 ng/ml to 2.05 ng/ml range), whereas T405 RIT was not ( $IC_{50} > 100$  ng/ml) (Figure 5a & b, Table 4a & b). In addition, T105 RIT (which targets a non-shed epitope) was the most active, even more active than the potent control RIT T6. (Note that because of the space limitations on the 96 well plate, it was not possible to test all four RITs and the T6 control in one plate. Hence, at least two assays were done for each cell line.) The cytotoxicity assay with the Atac4 cells ( $IC_{50}$  range 240 to 700 ng/ml ) confirmed that the cytotoxicity was specific to CD30+ cells (Figure 5c & d, Table 4a & b).

### **Cytotoxicity on HD and ALCL Derived Cell Lines**

The activity of T420 RIT, T427 RIT, T105 RIT, and T405 RIT was tested against a HD derived cell line (L540) and two ALCL derived cell lines (SUDHL-1 & Karpas 299). T6 dsFv RIT was also used as a positive control in these assays. The results were qualitatively similar to those in the A431/CD30 assay. T420 RIT, T427 RIT, and T105 RIT all had high degrees of cytotoxicity towards the SUDHL-1 ( $IC_{50}$  range 7.4 ng/ml to 19 ng/ml) and Karpas 299 ( $IC_{50}$  range 17 ng/ml to 60 ng/ml) (Figure 6, Table 4a & b). The RITs were also active against L540 cells but to a lesser degree ( $IC_{50}$  60 ng/ml to 105 ng/ml). T405 RIT was not active against Karpas 299 and SUDHL-1 ( $IC_{50} > 100$  ng/ml) and was not tested on the L540 cell line. Among all of these anti-CD30 dsFv RITs, T105 RIT which targets the non-shed epitope was consistently the most active in all of the CD30+ cell lines in every assay.



## **Measuring the Affinity of the Anti-CD30 dsFv IT towards CD30**

The affinities of the anti-CD30 dsFv RITs towards CD30-Fc on a biosensor chip was measured by surface plasmon resonance assay (See “Materials and Methods”). By measuring the on and off rates of the RIT binding to the CD30-Fc on the biosensor chip, the affinity was calculated (Kd). The Kd of T420 RIT, T427 RIT, T105 RIT, and T405 RIT were  $5.8 \times 10^{-8}$  M,  $3.6 \times 10^{-8}$  M,  $1.2 \times 10^{-8}$  M, and  $3.14 \times 10^{-7}$  M (Table 5). The RIT with the highest affinity, T105, also had the highest activity against CD30 positive cells. Conversely, the RIT with the lowest affinity, T405, had the lowest activity against CD30 cells. All of the RIT Fvs had lower affinities than the parent MABs they were based on, which was not unexpected considering that MABs are divalent and are generally in a more stable form. In addition, the parent MAB with the highest affinity, T427, did not have the highest affinity in the RIT Fv form.



## DISCUSSION

While combination chemotherapy and radiation therapy can achieve high remission rates in Hodgkin's Disease (HD), many of the patients who relapse will die from their disease (1,2,3). In addition, conventional therapy for Hodgkin's disease leads to several co-morbidities, including the development of secondary malignancies. Anaplastic large cell lymphoma (ALCL) is a novel category of lymphoma that has a cohesive proliferation of large pleomorphic blastic cells and consistently expresses the cytokine receptor CD30 (6). While the prognosis of ALCL varies depending on the subforms, there is a clinical need, as in HD, for more selective therapies.

HD and ALCL are clinically distinct, but they have many similarities. One of the most important of these similarities from the standpoint of designing a selective therapy is that both Reed-Sternberg cells (of Classic HD) and ALCL cells overexpress CD30. A number of attempts to target CD30 with MAbs and immunotoxins have been made. Although previous anti-CD30 RITs have demonstrated some effectiveness in *in vitro* assays and in animal models, a RIT with improved properties should have greater clinical efficacy. Two strategies were employed in attempting to develop an more effective RIT : 1) choosing parent MAbs with a high affinities to CD30 and 2) choosing parent MAbs that target epitopes in the non-shed portion of CD30. As mentioned in the introduction, CD30 is cleaved by a zinc-metalloprotease to produce a soluble fraction. CD30 also has multiple epitope groups, some of which are located on the non-shed portion of CD30 (Figure 2, S. Nagata - unpublished data). Targeting such epitopes has the advantage of : 1) having a greater number of binding sites available to the RIT and 2) not having the RIT neutralized by soluble CD30. Four novel anti-CD30 dsFv RITs (disulfide-stabilized Fv recombinant immunotoxins) were



produced based on two high affinity parent MAbs, T420 and T427, and two parent MAbs that target non-shed epitopes of CD30, T105 and T405. All four of the Fv's from these MAbs had unique sequences. Three of these RITs (T420, T427, T105) had a high degree of activity against CD30+ cells. Among these, T105 RIT was consistently the most active against each CD30+ cell line.

All four anti-CD30 dsFv RITs were produced with good yields (~5%). This is important for a number of reasons. Not all MAbs translate faithfully into an Fv form, so a good yield with high purity indicates stability of the Fv form. In addition, a good yield and high purity generally correlates with a highly active RIT. Another reason why yield and purity are important is that the best anti-CD30 dsFv RIT may be a candidate for clinical studies. Since producing RIT on a larger scale is a laborious and expensive process, it is important that the RIT can be produced with a reasonable yield. In addition, there are several strategies to improving the yield of a RIT which can be explored. One of these involves altering the conditions of the refolding process so that the RIT may aggregate less. Another approach is to use molecular modeling techniques to identify various framework residues which can be altered to produce an even more stable Fv configuration.

The four anti-CD30 RITs were tested on a panel of CD30+ cells, including those derived from HD and ALCL. While there were some differences in how effective they were in each cell line, three (T420, T427, and T105) of the RITs were generally very active in all of the CD30+ cell lines. Among these, T105 RIT, which targets a non-shed CD30 epitope was consistently the most active. The surface plasmon resonance assay revealed that the T105 RIT Fv also had the highest affinity towards CD30 among the anti-CD30 RITs. Since previous studies with RITs indicate that the affinity of the Fv to its target is one of the most





important factors in determining activity, T105's high activity may be explained by its high affinity to CD30 (35). Hence, it is unclear what the significance of T105 targeting a non-shed epitope is. Previous studies with anti-CD30 RITs did not find a relationship between RITs targeting different epitope groups within the shed region and their activity, but the non-shed region has not been explored before (35). As mentioned above, a RIT that targets a non-shed epitope should have several advantages. The idea that such a RIT should not be neutralized by soluble CD30 (sCD30) may be especially significant because it is believed that sCD30 may be dramatically elevated in a patient because it is shed in several places near a tumor site. However, it is difficult to replicate such conditions in an *in vitro* setting because the sCD30 released by the cells become quickly diluted by the media. It is also difficult to produce sCD30 in the quantities predicted in an *in vivo* setting and add it to an *in vitro* cytotoxicity assay to test the effects of neutralization of RITs that target shed epitope groups. Hence, it may only be possible of revealing the significance of targeting a non-shed epitope group through animal studies or through clinical studies.

While T420 RIT and T427 RIT were also highly active in CD30+ cells, they were not as active as predicted considering the high affinity of their parent MAb. Again, not all MAb translate faithfully into an Fv form. This was confirmed by the surface plasmon resonance assay which revealed that both of these RITs' Fvs had less affinity than their parent MAb. In addition, the lack of activity from the T405 RIT was surprising considering its good yield and high purity, which often correlate with strong activity. The surface plasmon resonance assay did reveal that the T405 RIT has significantly decreased affinity towards CD30, which may partially explain its low activity. Another interesting aspect of T405 RIT's structure is that its CDR3 in V<sub>H</sub> has only three amino acids, which is considerably shorter than most



CDR3s in immunoglobulins (Table 3). CDR3 usually plays a critical role in binding, but it is unclear what the significance of this short CDR3 may play in T405 RIT's lack of activity.

Within the CD30+ cell lines, there was a difference in their susceptibilities to the anti-CD30 RITs. It may be possible that these different cell lines express different levels of CD30, and this may play a role in how susceptible they are to RITs. This idea was explored in earlier studies, but surprisingly no relation between the CD30 expression and susceptibility to anti-CD30 RITs was found (35). There are other factors that play a role in how susceptible a given cell line may be to RITs. Some of these factors include the differences in internalization of the surface antigen (usually a receptor) and differences in how the toxin is processed once inside the cell. These other factors may explain the differences in the susceptibility of these cell lines.

Since the long-term objective is to develop an anti-CD30 therapeutic agent for clinical trials, future directions would involve further characterizing and development of the RIT(s) with the best specific activity. Future studies would include *in vitro* stability assays, pharmacokinetics ( $T_{1/2}$ ) studies, and toxicity ( $LD_{50}$ ) studies. In addition, the anti-tumor activity in a mouse subcutaneous tumor model will be measured. The RIT(s) with the most favorable properties can still be improved in several ways. Although the candidate RIT would already have high activity towards CD30, it is still possible to make a more active RIT by increasing the RIT's Fv's affinity through *in vitro* affinity maturation. While there are a number of approaches to affinity maturation (codon-based mutagenesis, CDR walking, error prone replication, and synthetic CDR construction), one of the most efficient methods is to mutagenize hot spots in the  $V_H$  and  $V_L$  of CDR3, which play a critical role in antigen binding. Using phage display technology, panning of hot spot mutant libraries using CD30+



cells should yield mutants with increased affinity. This strategy has been previously applied to other RITs with dramatic increases in affinity, activity and yield (44, 45). In addition, it may be possible to decrease the RIT's non-specific toxicity by lowering the isoelectric point (P<sub>I</sub>) of the Fv through mutation of exposed surface basic or neutral residues in the framework region to acidic residues (identified by molecular modeling). In another RIT, this approach resulted in a more than 2 fold decrease in non-specific toxicity in mice (46). While these earlier strategies involve improving the RIT itself, it is also worthwhile to investigate what conditions might increase the efficacy of the RIT. Since the antitumor effects of a RIT are affected by how many antigen binding sites are present on the tumor cell, agents (such as interferon gamma or IL-4) which may upregulate the expression of CD30 in malignant cells should be examined in *in vitro* cytotoxicity assays and in animal tumor models. Furthermore, previous studies with other RITs have demonstrated that chemotherapy can sensitize malignant cells to RITs (Pastan, unpublished data). Hence, animal tumor studies could be performed by pretreating animals with chemotherapy before applying the RIT. These combinations of strategies should optimize the candidate RIT(s) to have the greatest clinical efficacy.

If one of these novel anti-CD30 dsFv RITs is selected for clinical trials, it is important to consider how to incorporate it into a therapeutic regimen. RITs would be especially helpful in dealing with cancer cells that are chemotherapy resistant or in eliminating minimal residual disease. Another RIT developed in the Pastan lab (BL22) has been found to eliminate minimal residual disease in patients with chemotherapy resistant Hairy Cell Leukemia (24). Previous studies with anti-CD30 MAbs reveal that these antibodies do reach the tumor in most cases. Hence, RITs, which are smaller than IgG's, should be able to reach



tumor sites. Since chemotherapy has also been found to sensitize cancer cells to RITs, it would perhaps be most effective to include the anti-CD30 dsFv RITs with the typical chemotherapy regimen for HD or ALCL. By adding RITs to the chemotherapy regimen, the RITs may be able to eliminate chemotherapy resistant cells and minimal residual disease as well as decrease the doses of chemotherapy drugs needed, hence reducing the co-morbidities associated with them.





## References:

1. DeVita V.T. Jr., Serpick, A.A., Carbone, P.P. Combination chemotherapy in the treatment of advanced Hodgkin's Disease. *Ann. Intern. Med.*, 1970; 73(6): 881-95.
2. Longo, I.L., Young, R.C., Wesley, M, Hubbard, S.M., Duffy, P.L., Jaffe, E.S., DeVita, V.T. Jr. Twenty years of MOPP therapy for Hodgkin's lymphoma. *J. Clin. Oncol.*, 1986; 4: 1295-1306.
3. Greenlee RT, Murray T, Bolden S, Wingo PA. Cancer statistics, 2000. *CA Cancer J. Clin.*, 2000; 50: 7-33.
4. Tucker, MA, Coleman, C.N., Cox, R.S., Varghese, A., Rosenberg, S.A. Risk of second cancers after treatment of Hodgkin's disease. *N. Engl. J. Med.*, 1988; 318: 76-81.
5. Hancock, S.L., Tucker, M.A., Hoppe, R.T. Breast cancer after treatment of Hodgkin's disease. *J. Natl. Cancer Inst.*, 1993; 85: 25-31.
6. Stein H., Mason DY, Gerdes J., O'Connor, N. Wainscoat, J. The expression of the Hodgkin disease associated antigen Ki-1 in reactive and neoplastic lymphoid tissue: evidence that Reed-Sternberg cells and histiocytic malignancies are derived from activated lymphoid cells. *Blood*. 1985; 66: 848-58.
7. Stein, H., Foss, H-D., Durkop, H., Marafioti, T., Delsol, G., et. al. CD30+ anaplastic large cell lymphoma: a review of its histopathologic genetic, and clinical features. *Blood*, 2000; 96: 3681-3695.
8. Benharroch, D., Meguerian-Bedoyan, Z., Lamant, L., Amin, C., et. al. ALK-positive lymphoma: a single disease with a broad spectrum of morphology. *Blood*, 1998; 91:2076-84.
9. Falini, B., Bigerna, B. Fizzoti, M., Pulford, K., Pileri, S.A. et.al. ALK expression defines a distinct group of T/null lymphomas ("ALK lymphomas") with a wide range of morphological spectrum. *Am J Pathol.* 1998; 153:875-86.
10. Gascoyne, R., Aoun, P., Wu, D., Chhanabhai, M., Skinnider, B.F., et. al. Prognostic significance of anaplastic lymphoma kinase (ALK) protein expression in adults with anaplastic large cell lymphoma. *Blood*, 1999; 93: 3913-21.
11. Falini, B., Pileri, S., Zinzani, P.L., Carbone, A., Zagonel, V, et. al. ALK+ lymphoma: clinico-pathological findings and outcome. *Blood*, 1999; 93:2697-2706.



12. Durkop, H., Latza, U., Hummel, M., Eitelbach, F., Seed, B., Stein, H. Molecular cloning and expression of a new member of the nerve growth factor receptor family that is characteristic for Hodgkin's disease. *Cell*, 1992; 68:421-427.
13. Nawrocki, J.F., Kirsten, E.S., Fisher, R.I. Biochemical and structural properties of a Hodgkin's disease-related membrane protein. *J. Immunol.*, 1996; 141: 672-680.
14. Gruss, H.J., Boiani, N., Williams, D.E., Armitage, R.J., Smith, C.A., Goodwin, R.G. Pleiotropic effects of the CD30 ligand on CD30-expressing cells and lymphoma cell lines. *Blood*, 1994; 83: 2045-2056.
15. McDonald, P.P., Cassatella, M.A., Bald, A., Maggi, E., Raomagnami, S., et. al. CD30 ligation induces nuclear factor-kappa B activation in human T cell lines. *Eur J Immunol.*, 1995; 25:2870-2876.
16. Lee, S.Y., Lee, S.Y., Kandala, G., Liou, M-L., Choi, Y. CD30/TNF receptor-associated factor interaction: NF-kappa B activation and binding specificity. *Proc Natl Acad Sci.*, 1996; 93:9699-9703.
17. Horie, R., Watanabe, T. CD30: expression and function in health and disease. *Seminars in Immunology*. 1998; 10: 457-470.
18. Hansen, H.P., Kisselva, T., Kobarg, J., Horn-Lohrens, O, Havsteen, B., Lemke, H. A zinc metalloproteinase is responsible for the release of CD30 on human tumor cell lines. *Int J. Cancer*. 1995; 63: 750-756.
19. Zinzani, P.L., Pileri, S., Bernardi, M., Buzzi, M., Sabatini, E., Ascari, S., Gherlinzoni, F., et. al. Clinical implications of serum levels of soluble CD30 in 70 adult anaplastic large-cell lymphoma patients. *J. Clin. Oncol.*, 1998; 16: 1532-1537.
20. Pastan, I. Targeted therapy of cancer with recombinant immunotoxins. *Biochim. Biophys. Acta*, 1997; 1333: C1-C6.
21. Kreitman, R.J. Immunotoxins in cancer therapy. *Curr. Opin. Immunol*, 1999; 11: 570-578.
22. Kreitman, R.J., Wilson, W.H., White, J.D., Stetler-Stevenson, M., Jaffe, E.S., Giardina, S., Waldmann, T.A., and Pastan, I. Phase I trial of recombinant immunotoxin anti-Tac (Fv)-PE38 (LMB-2) in patients with hematologic malignancies. *J. Clin. Oncol.*, 2000; 18: 1622-1636.
23. Kreitman, R.J., Margulies, I., Stetler-Stevenson, M., Wang, Q.C., Fitzgerald, D.J., and Pastan, I. Cytotoxic activity of disulfide-stabilized recombinant immunotoxin



RFB4(dsFv)-PE38 (BL22) toward fresh malignant cells from patients with B-cell leukemias. *Clin. Cancer Res.*, 2000; 6: 1476-1487.

24. Kreitman, R.J., Wilson, W.H., Bergeron, K., Raggio, M., Stetler-Stevenson, M., Fitzgerald, D.J., and Pastan, I. Efficacy of anti-CD22 recombinant immunotoxin BL22 in chemotherapy-resistant hairy-cell leukemia. *N. Engl. J. Med.*, 2001; 345: 241-247.
25. Koon, H.B., Junghans, R.P. Anti-CD30 antibody-based therapy. *Current Opinion in Oncology*, 2000; 12: 588-593.
26. Gruss, H.J., Boiani, N., Williams, D.E., Armitage, R.J., Smith, C.A., et. al.. Pleiotropic effects of the CD30 ligand on CD30-expressing cells and lymphoma cell lines. *Blood*, 1994; 838: 2045-2056.
27. Tian, Z.G., Longo, D.L., Funakoshi, S., Asai, O., Ferris, D.K., et. al. In vivo tumor effects of unconjugated CD30 monoclonal antibodies on human anaplastic large-cell lymphoma xenografts. *Cancer Res.*, 1995; 55: 5335-5341.
28. Pfeifer, W., Levi, E., Petrogiannis-Halioitis, T., Lehmann, L., Wang, Z., et. al. A murine xenograft model for human CD30+ anaplastic large cell lymphoma: successful growth inhibition with an anti-CD30 antibody (HeFi-1). *Am J Pathol.*, 1999; 155: 1353-1359.
29. Wahl, A.F., Klussman, K., Thompson, J.D., Chen, J.H., Francisco, L.V., Risdon, G., et. al. The Anti-CD30 Monoclonal Antibody SGN-30 Promotes Growth Arrest and DNA Fragmentation *in Vitro* and Affects Antitumor Activity in Models of Hodgkin's Disease. *Cancer Research*, 2002; 62: 3736-3742.
30. Klimka, A., Barth, S, Matthey, B., Roovers, R.C., Lemke, H., Hansen, H., et. al. An anti-CD30 single –chain Fv selected by phage display and fused to Pseudomonas exotoxin A (Ki-4 (scFv)-ETA) is a potent immunotoxin against a Hodgkin-derived cell line. *Br J Cancer*, 1999; 80:1214-1222.
31. Barth, S., Huhn, M., Matthey, B., Tawadros, S., Schnell, R., Schinkothe, T., et. al. Ki-4 (scFv)-ETA', a new recombinant anti-CD30 immunotoxin with highly specific cytotoxic activity against disseminated Hodgkin tumors in SCID mice. *Blood*, 2000; 95: 3909-14.
32. Falini, B., Bolognesi, A., Flenghi, L., Tazzari, P.L., Broe, M.K., et. al. Response of refractory Hodgkin's disease to monoclonal anti-CD30 immunotoxin. *Lancet*, 1992; 339: 1195-1196.
33. Schnell, R., Staak, O., Borchmann, P., Schwartz, C., Matthey, B., Hansen, H., et. al. A Phase I Study with an Anti-CD30 Ricin A-Chain Immunotoxin (Ki-4.dgA)



in Patients with Refractory CD30+ Hodgkin's and Non-Hodgkin's Lymphoma. *Clinical Cancer Research*, June 2002; 8: 1779-1786.

34. Rozemuller, H., Chowdury, P.S., Pastan, I., Kreitman, R.J. Isolation of New Anti-CD30 scFvs from DNA-Immunized Mice by Phage Display and Biologic Activity of Recombinant Immunotoxins Produced by Fusion with Truncated *Pseudomonas* Exotoxin. *Int. J. Cancer*, 2001; 92:861-870.
35. Nagata, S., Onda, M., Numata, Y., Santora, K., Beer, R., Kreitman, R.J., Pastan, I. Novel Anti-CD30 Recombinant Immunotoxins Containing Disulfide-stabilized Fv Fragments. *Clinical Cancer Research*, July 2002; 8: 2345-2355.
36. Kabat, E.A., Wu, T.T., Perry, H.M., Gottesman, K.S., Foeller, C. Sequences of Proteins of Immunological Interest, 5<sup>th</sup> Ed. Bethesda, MD: U.S. Department of Health and Human Services, Public Health Service, NIH, Bethesda, 1991.
37. Reiter, Y., Brinkmann, U., Lee, B., and Pastan, I. Engineering antibody Fv fragments for cancer detection and therapy: disulfide-stabilized Fv fragments. *Nat. Biotechnol.*, 1996; 14: 1249-1245.
38. Ho, S.N., Hunt, H.D., Horton, R.M., Pullen, J.K., and Pease, L.R. Site-directed mutagenesis by overlap extension using the polymerase chain reaction. *Gene (Amst.)*, 1989; 77: 51-59.
39. Brinkmann, U., Reiter, Y., Jung, S.H., Lee, B., Pastan, I. A recombinant immunotoxin containing a disulfide-stabilized Fv fragment. *Proc. Natl. Acad. Sci.*, USA, 1993; 90: 7538-7542.
40. Buchner, J., Pastan, I., Brinkmann, U. A method for increasing the yield of properly folded recombinant fusion proteins: single-chain immunotoxins from renaturation of bacterial inclusion bodies. *Anal. Biochem.*, 1992; 205: 263-270.
41. Rozemuller, H., Chowdhury, P.S., Pastan, I., Kreitman, R.J. Isolation of new anti-CD30 scFvs from DNA-immunized mice by phage display and biologic activity of recombinant immunotoxins produced by fusion with truncated pseudomonas exotoxin. *Int. J. Cancer*, 2001; 92: 861-870.
42. Kreitman, R.J., Bailon, P., Chaudhary, V.K., Fitzgerald, D.J., Pastan, I. Recombinant immunotoxins containing anti-Tac(Fv) and derivatives of *Pseudomonas* exotoxin produce complete regression in mice of an interleukin-2 receptor-expressing human carcinoma. *Blood*, 1994; 83: 426-434.
43. Reiter, Y., Brinkmann, U., Jung, S.H., Lee, B., Kasprzk, P.G., King, C.R., Pastan, I. Improved binding and antitumor activity of a recombinant anti-erbB2 immunotoxin by disulfide stabilization of the Fv fragment. *J. Biol. Chem.*, 1994; 269: 18327-18331. Benharroch, D., Meguerian-Bedoyan, Z., Lamant, L., et. al.,





ALK-positive lymphoma: a single disease with a broad spectrum of morphology. *Blood*, 1998; 91:2076.

44. Chowdury, P.S., Pastan, I. Improving antibody affinity by mimicking somatic hypermutation *in vitro*. *Nat Biotechnol.*, 1999 Jun; 17(6): 568-72.
45. Beers, R., Chowdury, P., Bigner, D., Pastan, I. Immunotoxins with increased activity against epidermal growth factor receptor vIII-expressing cells produced by antibody phage display. *Clin. Cancer Res.*, 2000 Jul; 6(7): 2835-43.
46. Onda, M., Nagata, S., Tsutsumi, Y., Vincent, J.J., Wang, Q, et. al. Lowering the isoelectric point of the Fv portion of recombinant immunotoxins leads to decreased nonspecific animal toxicity without affecting antitumor activity. *Cancer Res.*, 2001 Jul; 61(13): 5070-71.



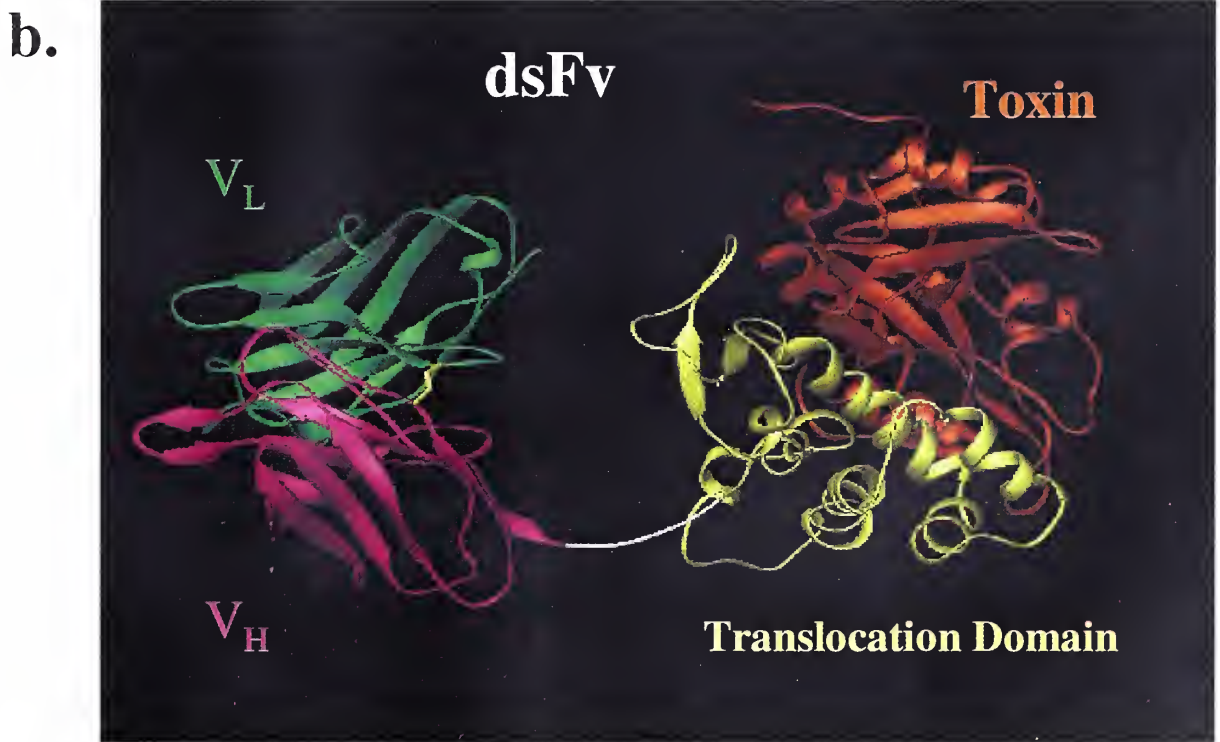
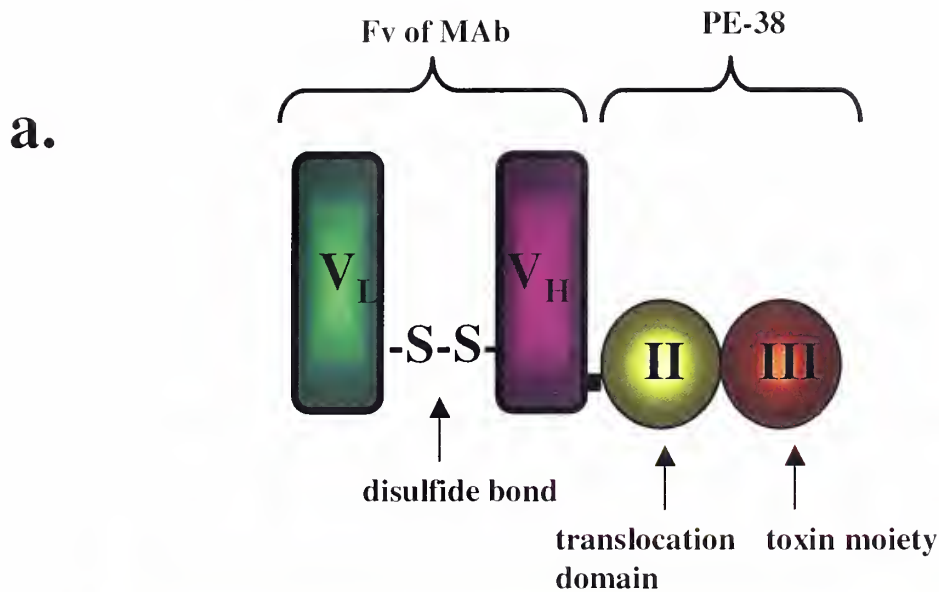


Figure 1a. Diagram of a disulfide-stabilized recombinant immunotoxin (dsFv RIT). Note that  $V_L$  is covalently bonded to  $V_H$  by a disulfide bond.  $V_H$  is fused to a modified *Pseudomonas* exotoxin (PE-38, 38 in size of the modified toxin in kDa). A *Pseudomonas* exotoxin typically has three domains: 1. a binding domain, 2. a translocation domain, 3. toxin moiety. In the RIT, the binding domain is replaced with the Fv of a MAb that targets a surface tumor antigen.

1b. A three dimensional molecular model of a dsFv RIT. (created by the Molecular Modeling Section of the Laboratory of Molecular Biology, NCI, NIH)



**Table 1: Parent MAb's for Anti-CD30 Recombinant Immunotoxins (RITs)**

Parent MAb	Isotype Subclass (of VH)	Affinity to CD30 Kd (nm)*	Epitope Group	Shed vs. Non-shed Epitope Target
T420	$\gamma$ 2b	1.9	I	shed
T427	$\gamma$ 2a	0.9	III	shed
T105	$\gamma$ 1	4.2	II	non-shed
T405	$\gamma$ 2b	5.7	VI	non-shed

Affinity measurements and epitope characterization done by Satoshi Nagata of the Pastan Lab, unpublished data)

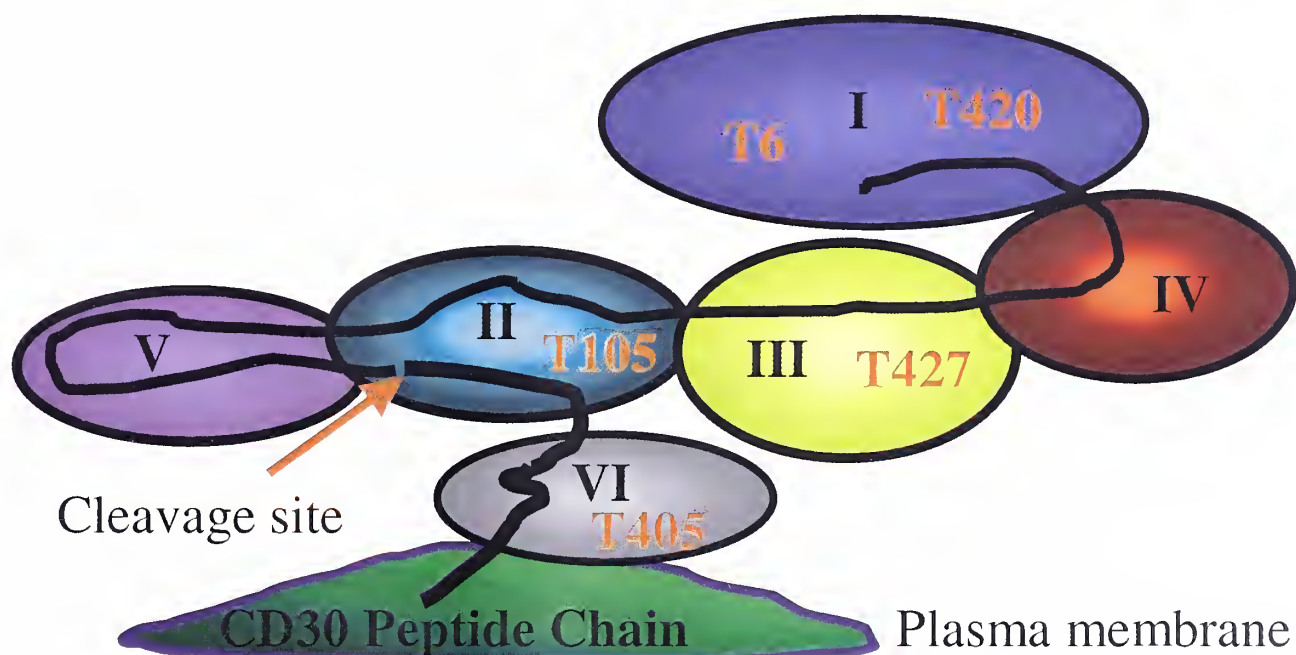


**Figure 2. Proposed topographical map of CD30 epitope groups determined by mutual competition assay (data not shown, done by Satoshi Nagata of the Pastan lab). There are six major epitope groups, each labeled with a Roman numeral. Note that T105 and T405 bind to epitopes that are in the non-shedding portion of CD30. T420 and T427 both bind to epitopes in the shed portion. T6 is a control anti-CD30 dsFv RIT.**



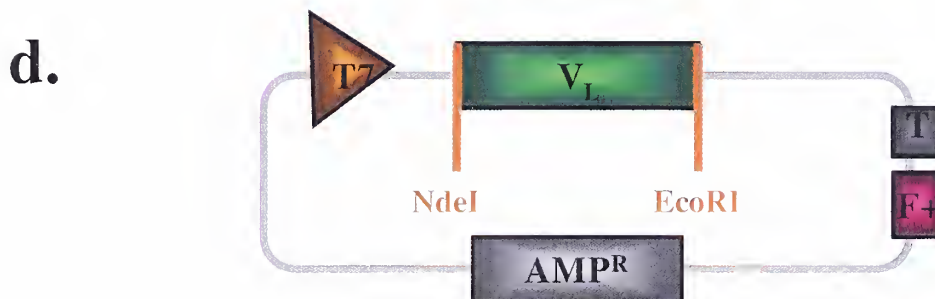
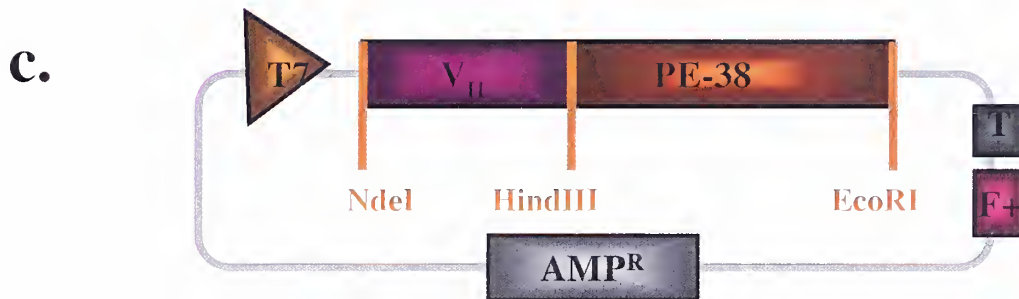
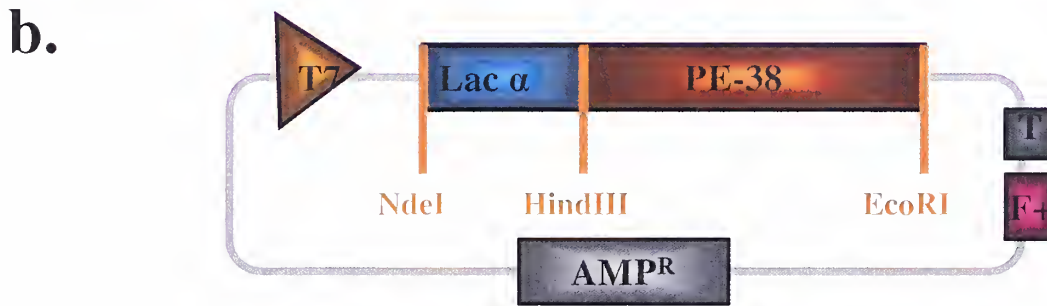
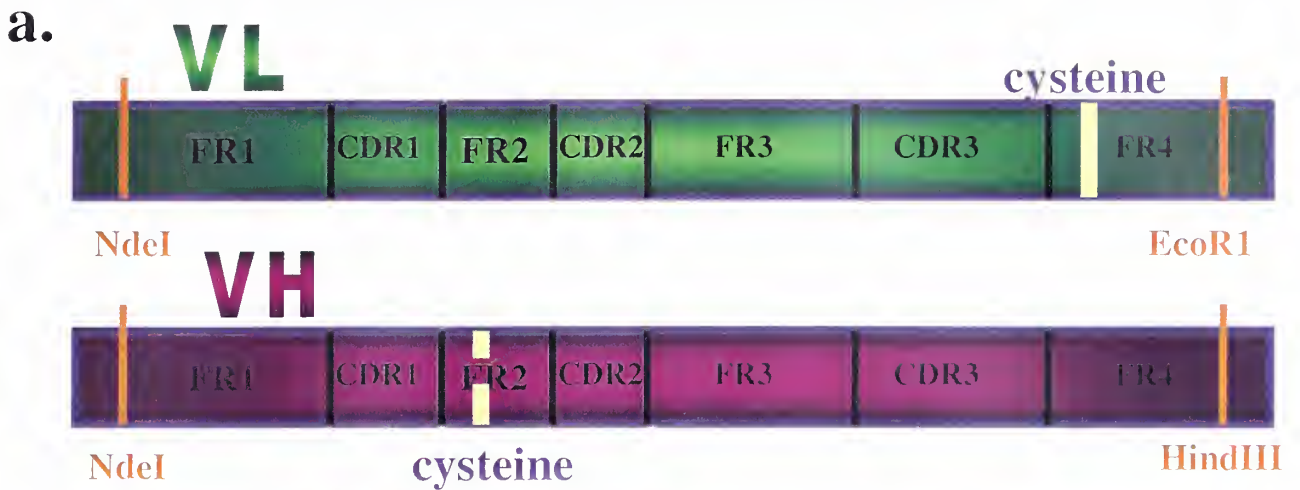


Figure 3a. A diagram of  $V_L$  (variable domain of the light chain) and  $V_H$  (variable region of the heavy chain)cDNA with cysteine mutations introduced and restriction sites added to the 5' and 3' end (to allow integration into the expression vector). A cysteine mutation was engineered in position 100 (framework region 4) for  $V_L$  and in position 44 (framework region 2) for  $V_H$ . (FR = framework region, CDR = complementary determining region). The cysteine mutations allow  $V_L$  to form a disulfide bond with  $V_H$  during the refolding process.

3b. Expression plasmid with PE-38 under a T7 promoter used for RIT production.

3c. Expression vector for  $V_H$ . Note that  $V_H$  is fused to a modified *Pseudomonas* exotoxin (PE-38).

3d. Expression vector for  $V_L$ .





**Table 2: Yields of the four anti-CD30 dsFv RITs. Minimal acceptable yield is 1%. A yield of 5% or greater is desirable.**

dsFv RIT	yield (%)
T420	4.27
T427	5.18
T105	5.58
T405	5.85

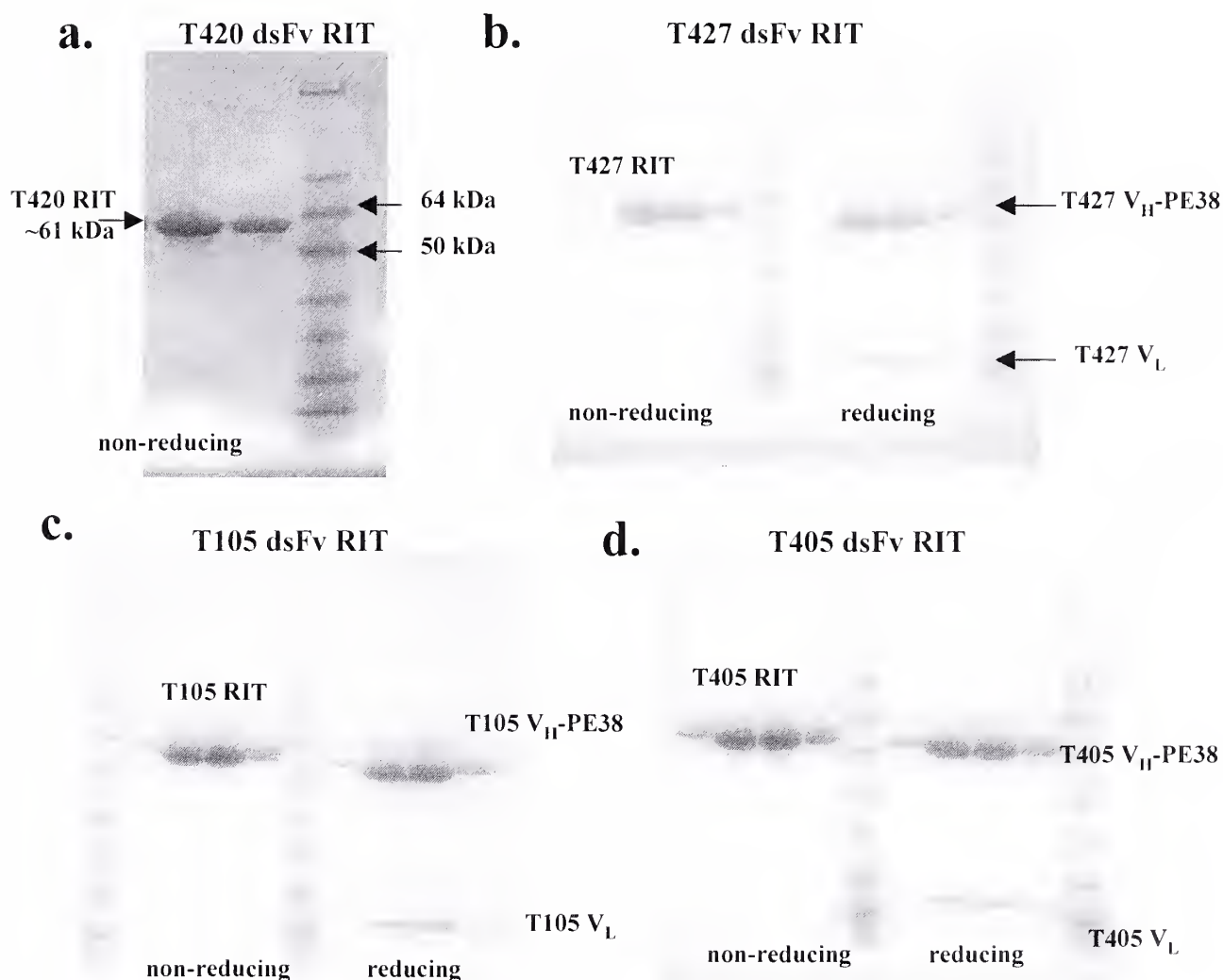


**Figure 4. The four anti-CD30 dsFv RITs analyzed on SDS-Page gel (to confirm size and determine purity). 4a. T420 dsFv RIT is shown in a non-reducing gel. The protein shown is of correct size (~61 kDa) and is very pure. 4b. T427 dsFv RIT is shown here in non-reducing and reducing conditions. Reducing conditions cleaves the disulfide bond, separating V<sub>H</sub>-PE38 from V<sub>L</sub>. 4c. T105 dsFv is shown in both non-reducing and reducing conditions. 4d. T405 dsFv RIT is shown in non-reducing and reducing conditions.**



**Table 3 : Amino acid sequence of V<sub>H</sub> and V<sub>L</sub> domains. All of the V<sub>H</sub> and V<sub>L</sub> sequences are unique.**

	FR1	CDR1	FR2	CDR2	FR3	CDR3	FR4						
<b>VH</b>	-----	-----	-----	-----	-----	-----	-----						
	1	2	3	4	5	6	7						
	2	3	4	5	6	7	8						
	3	4	5	6	7	8	9						
	4	5	6	7	8	9	10						
	5	6	7	8	9	10	11						
	6	7	8	9	10	11	12						
T420	QVQLQQS	GAELAKPGASV	KMSCKASGYTFT	SYWMH	WVKQRPGQDLEWIG	YINP--STDYTDY	NQKFKD	KATLTADR	KSSSTAYMQLSS	LTSEDSAVYYCAT	RHYGSSYGF	-----AY	WGQGTLLVTVSA
T427	QVQLQQPGTE	LVRFPGASVKL	SCKASGFSFT	SYWMN	WVKQRPGQGLEWIG	MIHP--SDSE	TRLNQKFKD	RATLTVDK	SSSTAYMQLSS	PTSEDSAVYYCAS	EMDY	YFAM-----DY	WGQGTSVTVSS
T405	QVQLQQIGAE	LVRFPGASVKL	SCKASGYTFN	NYWIN	WVKQRPGQGLEWIG	NIYP--SDRS	NYNQKFKD	KATLTVDR	KPSSTAYMQLSS	PTSEDSAVYYCTL	GS-----	-----Y	WGQGTLLVTVSA
T105	QVTLKESG	PGLIQPSQTL	SLTCSFSGFSL	TSGMGVS	WIRQFSGKLEWLA	HIY---WDD	DKRYNPSLKS	RLTISKDT	SSNQVFLKI	TSVDTADTATYYICAR	RADGLY	FYL-----DV	WGAGTIVTVSS

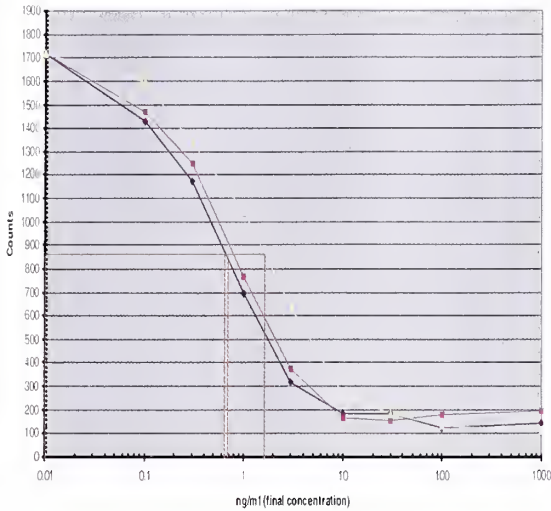
	FR1	CDR1	FR2	CDR2	FR3	CDR3	FR4									
	-----	-----	-----	-----	-----	-----	-----									
	1	2	3	4	5	6	7									
	2	3	4	5	6	7	8									
	3	4	5	6	7	8	9									
	4	5	6	7	8	9	10									
	5	6	7	8	9	10	11									
	6	7	8	9	10	11	12									
T420	DIVMTQSHK	EMSTSVGDRV	SITC	KASQ-----	DVSTAVA	WYQQKPGQSP	KLLIY	WASTRHT	GVPDRFTG	SGSGTDYSLT	ISSVQAEDLAVYYC	QQHYRTP	-----FT	FGSGTKLEIKR		
T427	DIVLTQSP	TSIAVSLGQR	ATISC	RASESVDS	-YGN	SFMH	WFQQKPGQSP	KLLIY	RASNLES	GIPARFSG	SGSWTDFTLT	INPVEAD	VDVATYYC	QQSNEDP	-----RT	FGGTKLEIKR
T405	DVVMQTPL	LSVTIGQP	ASLISC	KSSQSLSDS	-DGK	TYLN	WLLQRPQSP	KRLIY	LVSKLDS	GVPDRFTG	SGSGTDFTLK	ISRVEA	EDLGVYYC	WQGAHFP	-----RT	FGGTKLEIKR
T105	DIVMTQSK	EMSTSVGDRV	SVTC	KASQ-----	NVNTNVA	WYQQKPGQSP	EALIIY	SASRYYS	GVPDRFTG	SGSGTDFTLT	ISNVQSE	DLAEYFC	QQYNSYP	-----LT	FGSGTKLEIKR	

**VL**

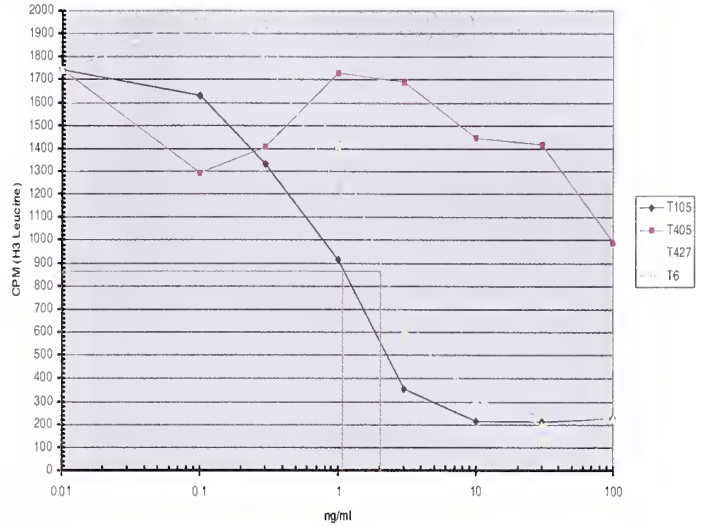


**a.**

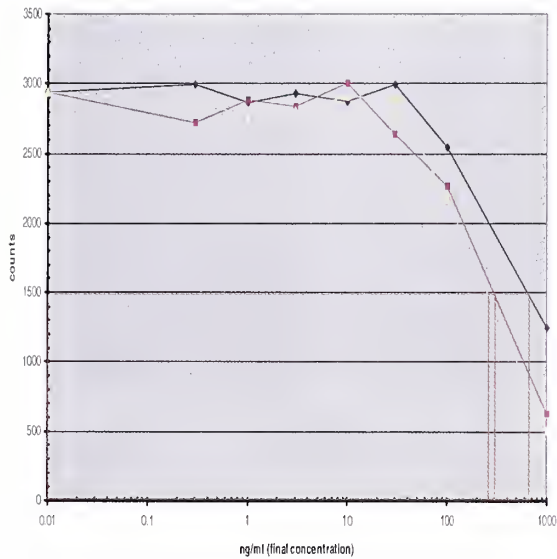
A431/CD30 Cells

**b.**

A431/CD30 Cells

**c.**

Atac4 cells (CD30-)

**d.**

Atac4 cells (CD30-)

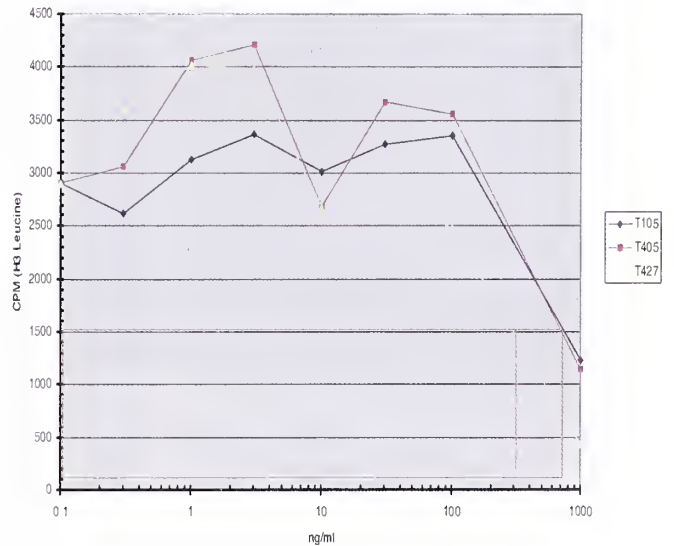


**Figure 5. *In vitro* Cytotoxicity assays of anti-CD30 dsFv RITs in A431/CD30 cells (a & b) and in Atac4 (CD30-) cells (c & d). The final concentration of the RIT in the media (ng/ml) is plotted against the counts per minute (CPM) of <sup>3</sup>H-Leucine (which correlates with cell count). The red bar indicates where the counts are 50% of the starting value and identify the IC<sub>50</sub> point.**

**5a. T105, T420, & T6 in A431/CD30 cells**

**5b. T105, T405, T427, & T6 in A431/CD30 cells**

**5c. T105, T420, T6 in Atac4 cells**

**5d. T105, T405, T427 in Atac4 cells.**



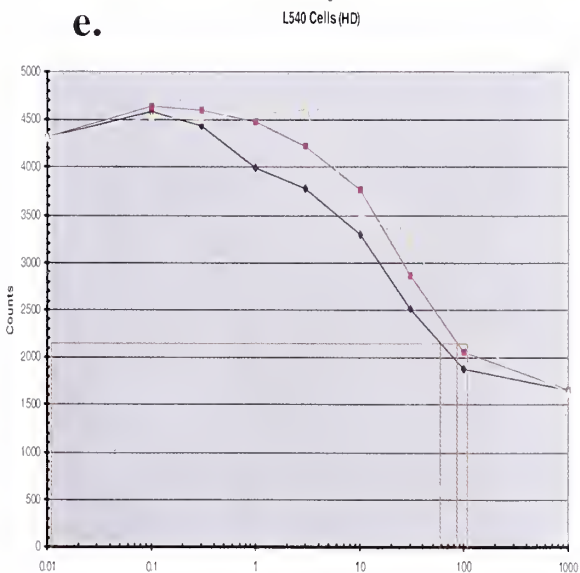
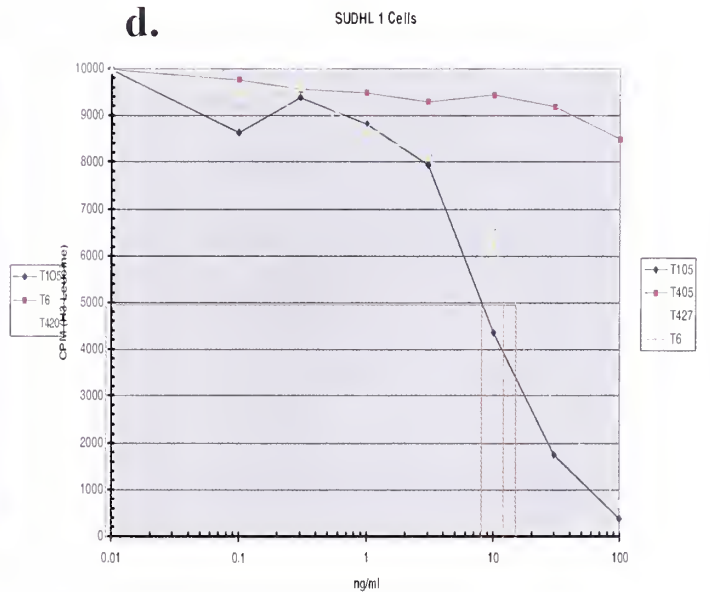
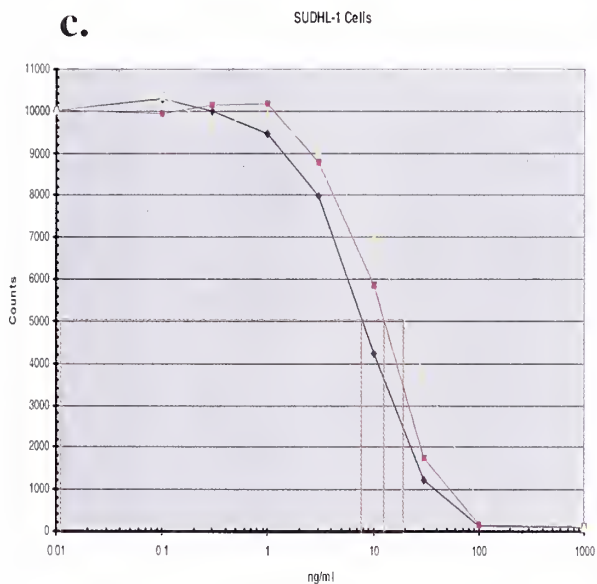
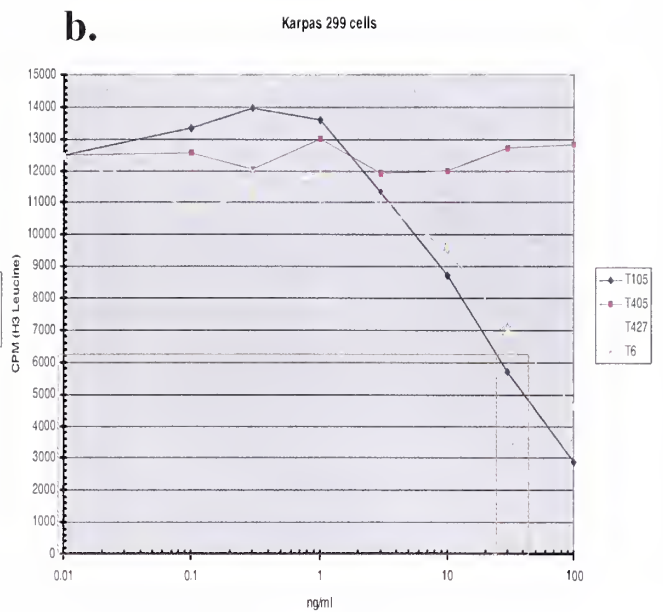
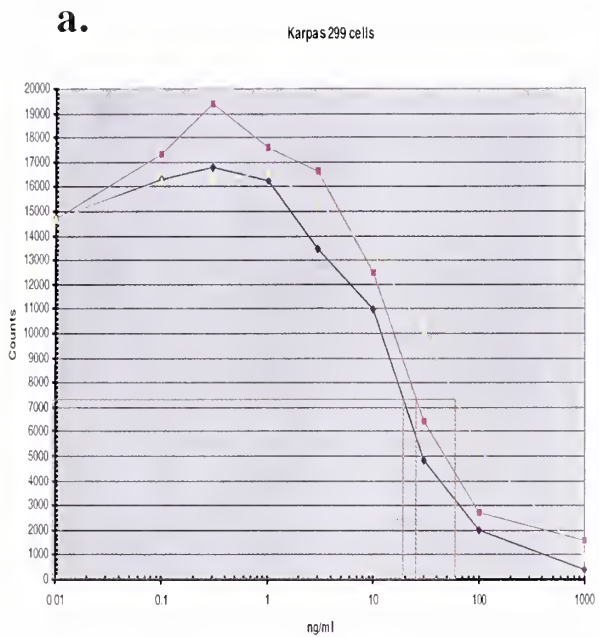


**Figure 6. *In vitro* cytotoxicity assays of anti-CD30 RITs in Karpas 299 (ALCL), SUDHL-1 (ALCL), and L540 (HD). The final conc. of RITs in media is plotted against counts per minute of  $^3\text{H}$ -Leucine. The red bar indicate where the counts are at 50% of the starting value and identify the  $\text{IC}_{50}$  point.**

**6a. T105, T420, & T6 in Karpas 299**

**6b. T105, T427, T405, & T6 in Karpas 299**

**6c. T105, T420, T6 in SUDHL-1**

**6d. T105, T427, T405, & T6 in SUDHL-1**

**6e. T105, T420 & T6 in L540**





**Table 4 (a & b): Summary of cytotoxicity studies of the anti-CD30 dsFv RIT in a number of different cell lines. IC<sub>50</sub> values of the RIT in each cell line is listed.**

**a.**

<b>Cell Line</b>	<b>T427 (IC<sub>50</sub>)</b>	<b>T405 (IC<sub>50</sub>)</b>	<b>T105 (IC<sub>50</sub>)</b>	<b>T6 (IC<sub>50</sub>) (control)</b>
<b>A431/CD30</b>	<b>2.05 ng/ml</b>	<b>&gt; 100 ng/ml</b>	<b>1.05 ng/ml</b>	<b>2 ng/ml</b>
<b>Karpas 299</b>	<b>41 ng/ml</b>	<b>&gt; 100 ng/ml</b>	<b>22 ng/ml</b>	<b>&gt;30 ng/ml (~40ng/ml?)</b>
<b>SUDHL-1</b>	<b>13 ng/ml</b>	<b>&gt; 100 ng/ml</b>	<b>8 ng/ml</b>	<b>11 ng/ml</b>
<b>Atac 4 (neg. control)</b>	<b>310 ng/ml</b>	<b>710 ng/ml</b>	<b>720 ng/ml</b>	<b>not included</b>

**b.**

<b>Cell Line</b>	<b>T420 (IC<sub>50</sub>)</b>	<b>T105 (IC<sub>50</sub>)</b>	<b>T6 (IC<sub>50</sub>)</b>
<b>Atac4 (CD30-)</b>	400 ng/ml	700 ng/ml	480 ng/ml
	240 ng/ml	640 ng/ml	300 ng/ml
<b>A431/CD30</b>	1.5 ng/ml	0.63 ng/ml	0.7 ng/ml
	1.9 ng/ml	0.73 ng/ml	0.8 ng/ml
<b>Karpas 299 (ALCL)</b>	53 ng/ml	17 ng/ml	20 ng/ml
	60ng/ml	19ng/lm	24ng/ml
<b>SUDHL-1 (ALCL)</b>	18 ng/ml	8 ng/ml	9.8 ng/ml
	19 ng/ml	7.4 ng/ml	11 ng/ml
<b>L540 (HD)</b>	105 ng/ml	60 ng/ml	90 ng/ml



**Table 5: Surface Plasmon Resonance Assay Results. The  $k_{on}$  and  $k_{off}$  rates were measured using BIAcore biosensor, and the  $K_d$  for each anti-CD30 dsFv RIT was calculated.**

<b>Anti-CD30 dsFv RIT</b>	<b><math>k_{on}</math> (1/MS)</b>	<b><math>k_{off}</math> (1/s)</b>	<b><math>K_d</math> (M) of RIT Fv</b>	<b>Affinity of Parent MAb (M)</b>
<b>T420</b>	<b><math>5.3 \times 10^4</math></b>	<b><math>3.0 \times 10^{-3}</math></b>	<b><math>5.8 \times 10^{-8}</math></b>	<b><math>1.9 \times 10^{-9}</math></b>
<b>T427</b>	<b><math>5.9 \times 10^4</math></b>	<b><math>2.1 \times 10^{-3}</math></b>	<b><math>3.6 \times 10^{-8}</math></b>	<b><math>0.9 \times 10^{-9}</math></b>
<b>T105</b>	<b><math>6.1 \times 10^4</math></b>	<b><math>7.4 \times 10^{-4}</math></b>	<b><math>1.2 \times 10^{-8}</math></b>	<b><math>4.2 \times 10^{-9}</math></b>
<b>T405</b>	<b><math>2.7 \times 10^4</math></b>	<b><math>8.6 \times 10^{-3}</math></b>	<b><math>3.14 \times 10^{-7}</math></b>	<b><math>5.7 \times 10^{-9}</math></b>











**HARVEY CUSHING/JOHN HAY WHITNEY  
MEDICAL LIBRARY**

**MANUSCRIPT THESES**

Unpublished theses submitted for the Master's and Doctor's degrees and deposited in the Medical Library are to be used only with due regard to the rights of the authors. Bibliographical references may be noted, but passages must not be copied without permission of the authors, and without proper credit being given in subsequent written or published work.

This thesis by  
has been used by the following person, whose signatures attest their acceptance of the above restrictions.

---

---

**NAME AND ADDRESS**

**DATE**

YALE MEDICAL LIBRARY



3 9002 01061 6986

